Langmuir

Article

pubs.acs.org/Langmuir

Surface Chemistry of Thiomalic Acid Adsorption on Planar Gold and Gold Nanoparticles

Julio C. Azcárate,[†] María Alejandra Floridia Addato,[†] Aldo Rubert,*[,†] Gastón Corthey,[†] Germán S. Kürten Moreno,[†] Guillermo Benítez,[†] Eugenia Zelaya,[‡] Roberto C. Salvarezza,[†] and Mariano H. Fonticelli*[,†]

[†]The Research Institute of Theoretical and Applied Physical Chemistry (INIFTA), National University of La Plata - CONICET, Sucursal 4 Casilla de Correo 16, 1900 La Plata, Argentina

[‡]Bariloche Atomic Center, National Atomic Energy Commission - CONICET, Av. Bustillo 9500, 8400 S. C. de Bariloche, Río Negro Argentina

Supporting Information

ABSTRACT: The self-assembly of thiomalic acid (TMA) on Au(111) and on preformed Au nanoparticles (AuNPs) protected by weak ligands has been studied by X-ray photoelectron spectroscopy (XPS) and electrochemical techniques. Results show that TMA is adsorbed on the Au(111) surface as thiolate species with a small amount of atomic sulfur (~10%) and a surface coverage lower than that found for alkanethiols due to steric factors. The amount of atomic sulfur markedly increases when the TMA is adsorbed on AuNPs by the ligand exchange method. We propose that the atomic sulfur is produced as a consequence of C−S bond cleavage, a process that is more favorable at defective sites of the AuNPs surface. The bond scission is also assisted by the presence of the electron-withdrawing carboxy moiety in the α-position relative to the C−S bond. Moreover, the high local concentration of positively charged species increases the stability of the negatively charged leaving group, leading to a higher amount of coadsorbed atomic sulfur. Our results demonstrate that the terminal functionalities of thiols are conditioning factors in the final structure and composition of the adlayers.

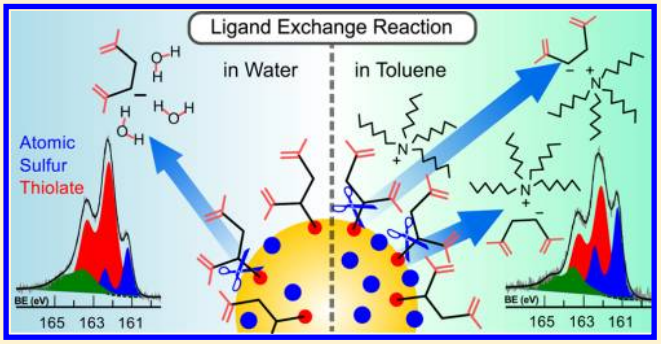

INTRODUCTION

In recent years, self-assembled monolayers (SAMs) of ω-terminated alkanethiols have been widely employed as linkage layers to electrostatically or covalently bind redox proteins to metal surfaces.[1] In this regard, thiomalic acid (TMA) belongs to the hydrophilic thiols that can serve as adhesion layers for biomolecules[2] and cells to study their chemical and electrochemical reactivity at interfaces. Also, the TMA molecule is an intriguing choice to protect nanoparticles intended for biomedical applications because of its water solubility, biocompatibility, and *in vivo* stability.[3]

The strong Au−S bond in thiolate-protected AuNPs imparts superior stability to the particles.[4,5] In the case of the TMA molecule the two carboxylic acid groups would also offer strong intermolecular hydrogen bonding. Thus, good water solubility is expected, besides the possibility to conjugate the particles through covalent bonding. Indeed, TMA can also stabilize nanoparticles in weak acidic solution.[3] However, if TMA-protected Au particles are synthesized in a single-phase system, based on the reduction of hydrogen tetrachloroaurate(III) by sodium borohydride in methanol,[6] partial reduction of the polymeric Au(I)−thiolate intermediate takes place.[7] As previously demonstrated, this synthesis strategy leads to gold@gold(I)thiomalate core@shell particles.[8] Although we have carried out some improvements by slightly changing the original synthesis by Chen and Kimura,[6] it was not possible to completely reduce the Au(I) polymeric species.

In order to obtain AuNPs protected by TMA (AuNP@TMA) without a polymeric shell of gold(I) species, we performed ligand exchange reactions on Au nanoparticles protected by labile ligands. We demonstrate that the AuNP@TMA are extremely stable in aqueous solutions, as they can be dispersed in a wide range of pHs, from 1 to 13. Although the AuNP@TMA represents a stable and robust system, there are intriguing aspects with regards to their surface chemistry that have to be assessed.

In this work we have made a comparative study of TMA self-assembly on Au(111) and AuNPs prepared by the ligand exchange reaction in solution to understand the process that controls the surface chemistry and structure of TMA-protected AuNPs. Our results demonstrate that the ligand-exchange method leads to monolayer protected AuNPs avoiding TMA−

Received: December 4, 2013
Revised: January 23, 2014
Published: January 30, 2014

   dx.doi.org/10.1021/la404674m | *Langmuir* 2014, 30, 1820−1826

Au(I) polymer formation. TMA assembles both on nanoparticles and on Au(111) surfaces. However, a significant amount of atomic S is present on AuNPs, suggesting an efficient C−S bond cleavage at defective-site-rich surfaces. We explain this stressing the importance of the terminal group in determining the chemistry and structure of thiol SAMs. Besides ligand exchange reactions lead to atomic sulfur and thiolates as coadsorbates, as the traditional synthesis does, we demonstrate that the amount of atomic sulfur seems to depend on the nature of the medium and the species dissolved in it.

EXPERIMENTAL SECTION

Chemicals. $HAuCl_4$ (Aldrich #50778, 25 mM in HCl 0.1 M), propanethiol (PT), thiomalic acid (TMA, >99%, Fluka #88460), tetrakis(hydroxymethyl)phosphonium chloride (THPC, solution 80% in water, Aldrich #404861), tetraoctylammonium bromide (TOABr, 98%, Aldrich #294136), sodium borohydride (≥99%, Aldrich #71321), absolute ethanol (Carlo Erba), toluene (Carlo Erba), and Milli-Q water. All chemicals were purchased from commercial suppliers and were used as received without further purification.

Synthesis of Gold Nanoparticles Capped by TMA (AuNP@TMA). AuNP@TMA were prepared by ligand exchange reactions performed over two different kinds of nanoparticles from aqueous or organic (toluene) media. The water-soluble nanoparticles (AuNP@THP) were capped by trihydroxymethylenephosphine, while the toluene-soluble ones (AuNP@TOABr) were protected by tetraoctylammonium bromide. We denoted by THP-AuNP@TMA the nanoparticles obtained from ligand exchange reaction in water solution and by TOABr-AuNP@TMA those modified in toluene solution.

AuNP@THP. The synthesis of these hydrosol nanoparticles has been developed by Duff et al.[9] Briefly, 3 mL of freshly prepared NaOH aqueous solution (0.3 mmol) was added to 44 mL of Milli-Q water. Then 1 mL solution of THPC (0.05 mol) was taken from a diluted THPC solution (1.2 mL, 80% of THPC in 100 mL of water) and was mixed with the alkaline solution in a round-bottom flask with a magnetic stir. After 2 min, 2 mL (0.05 mol) of $HAuCl_4$ aqueous solution was added. The pale yellow mixture turned brown after 30 s, leading to 3−4 nm gold nanoparticles capped with trihydroxymethylenephosphine (AuNP@THP).

AuNP@TOABr. These hydrophobic nanoparticles were synthesized by the biphasic method developed by Schiffrin et al.[10] An aliquot of $HAuCl_4$ aqueous solution (0.2 mmol of Au(III) in 20 mL) was mixed with a tetraoctylammonium bromide (TOABr) solution in toluene (0.8 mmol of TOABr) in order to transfer Au(III) species to the nonpolar phase of toluene. The mixture was stirred until the aqueous phase became colorless. After that, this phase was discarded. A sodium borohydride solution was added as reducing agent (2 mmol in 5 mL of water). The toluene phase turned dark red with gas evolution. The reaction media was further stirred for 2 h. The aqueous phase was discarded, and the toluene phase was washed with water.

Ligand Place Exchange Reactions. The reactions were carried out using a 2:1 Au:TMA molar ratio to minimize possible changes in the average size of Au core under ligand excess.[11] In a typical procedure an appropriate amount of TMA was dissolved in ethanol to obtain a concentrated solution. The volume of ethanol solution used in each case was lower than 5% of the AuNP solution. The reaction mixture was stirred overnight.

AuNP@THP increase their size over time, showing changes in their color. Indeed, the UV−vis spectroscopy data show an increase in the plasmon peak intensity at ∼520 nm and a red-shift as time progresses.[9] On the other hand, when TMA is added as capping agent, it effectively quenches the growth of nanoparticles. Interestingly, the THP-AuNP@TMA showed no evident changes in the UV−vis spectra over 6 months. The average diameter of these nanoparticles determined by transmission electron microscopy (TEM) was 3.7 ± 0.9 nm (see Supporting Information).

The mixture of the toluene phase of AuNP@TOABr and the TMA ethanolic solution leads to a black precipitate of Au nanoparticles (TOABr-AuNP@TMA). The supernatant was discarded, and the pellet was rinsed with toluene and ethanol (two times) and precipitated with a centrifuge (∼2000*g*). The average diameter determined by TEM was 4.4 ± 0.6 nm (see Supporting Information). Then, the TOABr-AuNP@TMA were dissolved in 0.1 M NaOH aqueous solution.

Preparation and Electrochemical Characterization of SAMs on Au(111). Preferred oriented (111) evaporated Au on glass were used as substrates (AF 45 Berliner Glass KG, Germany) for the study of TMA adsorption on planar surfaces. After annealing for 10 min with a hydrogen flame, these Au substrates exhibit atomically smooth (111) terraces separated by monatomic steps.

The electrochemical measurements have been carried out by means of an operational amplifier potentiostat (TEQ-Argentina). A saturated calomel electrode (SCE) and a large-area platinum foil were used as reference and counter electrode, respectively. All potentials in the text are referred to the SCE scale. The real surface area of working electrodes was determined by measuring the charge needed to reduce a gold oxide monolayer, which is a two-electron process. This was done by integrating the main cathodic peak in the current−potential curves obtained in 0.1 M $HClO_4$ aqueous solutions between 0.0 V versus a reversible hydrogen electrode (RHE) and the so-called Burshtein minimum.[12] The roughness factor average was 1.18 ± 0.03.

After surface preparation the Au substrates were immersed in 5×10^{-5} M thiol (TMA or propanethiol, PT) solutions overnight to yield a complete SAM and then rinsed carefully with pure solvent to remove weakly adsorbed molecules. The samples were kept in the dark during immersion in order to avoid photo-oxidation. Absolute ethanol, water, and toluene were used as solvents in the modification of Au(111) surfaces with TMA.

Some of the TMA-covered substrates were then analyzed by X-ray photoelectron spectroscopy (XPS) while other samples were placed in an electrochemical cell containing 0.1 M NaOH to carry out thiol electrodesorption experiments and thus determine the electrodesorption potential, E_p. Electrodesorption curves were recorded at 0.050 V s^{-1}. The 0.1 M NaOH aqueous solution used as the base electrolyte was prepared from solid NaOH (analytical grade from Baker). In all cases the solutions were prepared with Milli-Q water. The electrolyte was thoroughly deaerated by bubbling with nitrogen prior to each experiment. All measurements were performed at room temperature.

Transmission Electron Microscopy. TEM imaging of AuNPs was performed using a FEI CM200 UT microscope, operating at 200 kV. The images were taken with the nanoparticles supported on 300 mesh ultrathin carbon film on holey carbon support copper grids. The size distribution of nanoparticles was performed using ImageJ software[13] by measuring more than 100 nanoparticles from bright-field images. A log-normal distribution function was fitted to the histogram obtained, according to ref 14 (see Supporting Information).

X-ray Photoelectron Spectroscopy. The samples were characterized by XPS using a Mg Kα source (XR50, Specs GmbH) and a hemispherical electron energy analyzer (PHOIBOS 100, Specs GmbH). A two-point calibration of the energy scale was performed using sputtered cleaned gold (Au $4f_{7/2}$, binding energy (BE) = 84.00 eV) and copper (Cu $2p_{3/2}$, BE = 932.67 eV) samples. XPS was also performed at the PGM beamline of the Laboratório Nacional de Luz Síncrotron (LNLS), Campinas, Brazil, with a hemispherical electron energy analyzer (PHOIBOS 150, Specs GmbH). The energy of the incident photons ($h\nu$) was set to 250 and 523 eV, with fluxes of 1×10^{14} and 2×10^{14} photon s^{-1} cm^{-2}, respectively. For the synchrotron-based measurements, the BE scale was corrected by fitting the XPS data near the Fermi level (see Supporting Information). Also, a dodecanethiol SAM on Au(111) was used as reference. For this sample the Au $4f_{7/2}$ peak was located at 83.92 eV, which is very close to the ISO standard value of 83.95 eV.[15] Notably, the full width at half-maximum (fwhm) for the Au $4f_{7/2}$ peak for this SAM is ∼0.5 eV. Special care was taken to avoid radiation damage. Indeed, the measurements performed at PGM beamline were carried out in a

dx.doi.org/10.1021/la404674m | *Langmuir* 2014, 30, 1820−1826

single scan. The effect of radiation damage on the samples has been carefully analyzed, as illustrated in the Supporting Information.

Density Functional Theory (DFT) Vibrational Frequency Calculation. We used Gabedit[16] software as user interface to generate input files and read output files for MOPAC2012[17] and MPQC[18,19] computational chemistry package. First, geometry optimization was carried out by semiempirical method with MOPAC2012 using a PM6[20] Hamiltonian. Then, geometries were reoptimized and frequencies were calculated using B3LYP density functional with a 6-31+G* basis set by using the MPQC package.

RESULTS AND DISCUSSION

Electrochemical Data of TMA Adsorption on Au(111). The stability of thiolate SAMs as well as their surface coverage can be assessed by electrochemical methods. Figure 1a displays

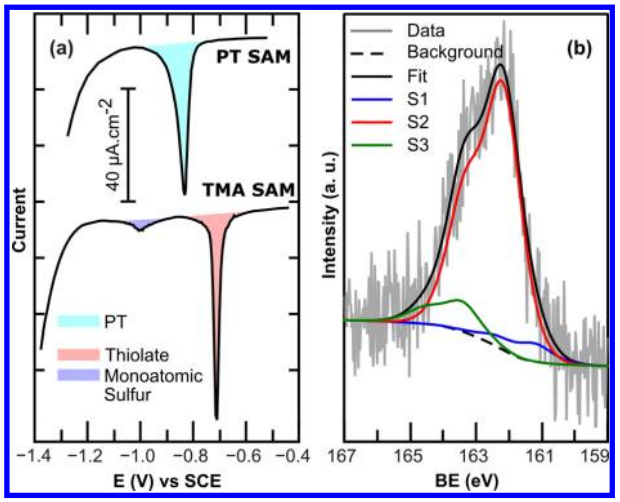

Figure 1. (a) Cathodic polarization curves recorded for PT (upper trace) and TMA (lower trace) on Au(111) in 0.1 M NaOH. Scan rate 0.050 V s^{-1}. (b) S 2p XPS spectrum of a Au(111) surface modified by TMA.

typical electrodesorption curves recorded for TMA and PT-covered Au electrodes where the main cathodic current peaks correspond to the well-known thiol reductive desorption reaction.[21] The massive desorption of the TMA monolayer occurs at $E < -0.6$ V with the peak potential located at $E_p = -0.7$ V. On the other hand, the reductive desorption of PT occurs massively at $E < -0.8$ V with $E_p = -0.83$ V. The amount of charge, q, involved in the reductive desorption peaks gives information about the thiol coverage. For TMA ($q_{TMA} = 0.049 \pm 0.005$ mC cm^{-2}) this magnitude results smaller than for propanethiol ($q_{PT} = 0.071$ mC cm^{-2}). Considering that 0.074 mC cm^{-2} [22] is the expected charge for a Au(111)-($\sqrt{3} \times \sqrt{3}$)$R30°$-PT lattice, the surface coverage of TMA results in $\theta_{TMA} = 0.22$. This is reasonable since one would expect TMA to have a lower coverage than PT as a consequence of steric hindrance of TMA related species. Note that if the potential is reversed in the positive direction (not shown in Figure 1), no evidence of PT and TMA readsorption is observed, indicating that the desorbed species are soluble in the alkaline solution.

The fact that the E_p value for PT is more negative than for TMA is a sign of higher stability of the PT SAM. This can be explained considering the repulsive interactions between the carboxylate groups in the alkaline solution, which are not completely neutralized by the counterions.[12,23] Also, the solvation of thiomalate anion might be more favorable than that of propanethiolate.

These results indicate the formation of thiolate monolayers upon exposure of the clean Au surfaces to the thiol solutions. On the other hand, the features observed at $-0.9 > E > -1.0$ V are too negative to be related to desorption of residual thiolate species of a short thiol. Alternatively, we could relate this to a small amount of atomic sulfur, a possible coadsorbate in thiol adsorption.[24] This consideration is supported by XPS analysis (see below). The desorption of diluted atomic sulfur takes place by the well established two-electron electrochemical reaction.[25] The amount of charge related to this reaction was $q_S = 0.010$ mC cm^{-2}, which corresponds to a surface coverage of $\theta_S = 0.02$.

XPS Analysis of TMA Adsorption on Au(111). The chemical nature of the adsorbates has been assessed by XPS. Figure 1b shows the S 2p region of the XPS spectrum of a TMA-modified Au(111) substrate. The absolute value of the BE of the S $2p_{3/2}$ is employed to obtain information about the chemical bonding of the S to the Au surface. The S $2p_{3/2}$ core level peak for SAMs of thiols on Au can be decomposed into three different components: S1 and S2 near 161 and 162 eV, respectively, and S3 at 163−164 eV.[26] The S1 component is associated with atomically adsorbed sulfur species.[24,27] The S2 component is related to S chemisorbed on the metal surface through a thiolate bond, while the S3 component has been assigned both to unbound thiol and disulfide species.[28−30] In Figure 1b, the more abundant component is that corresponding to thiolate, while S1 represents ∼10% of the area below the curve of the S2 component. For our experimental setup, the ratio $S_{thiolate}$/Au results in 0.056 for a compact SAM of alkanethiol with a surface coverage of $\theta = 1/3$.[31] Instead of that, we found a S/Au atomic ratio of 0.0026 for S1 and 0.039 for S2, which correspond to $\theta_{S1} = 0.02$ and $\theta_{S2} = 0.23$. These figures are in good agreement with the electrochemical results and reinforce previous claims about the influence of the thiol nature on the final structure of the SAM. In fact, recent studies on the determination of thiol ligand density on AuNPs postulate sterical hindrance as a conditioning factor on the expected surface coverage.[32,33]

XPS Analysis of TMA-Modified Gold Nanoparticles. TMA-modified gold nanoparticles (AuNP@TMA) were prepared by ligand exchange reaction to avoid the formation of Au(I)−TMA polymer obtained by the traditional one-phase synthesis.[8] The ligand-exchange reactions have common features with the processes involved in SAM formation onto bulk surfaces. However, if the ligand-exchange reaction was carried out in the presence of high excess of thiols, Au(I)−thiolate complexes would be formed due to the extensive etching of metallic cores.[34] The analysis of the Au 4f signal obtained with incident X-rays of 250 and 523 eV showed that no Au(I) species are present (Figure 2). Indeed, the BE of the Au $4f_{7/2}$ peak was centered between 83.88 and 83.99 eV, near the value found for dodecanethiolate SAMs on bulk Au, and the fwhm was 0.60−0.66 eV. Note that when the photon energy is 250 eV, the analyzed depth is about 1−2 atomic layers of Au, while for 523 eV 2−3 atomic layers contribute to the XPS signal.[35,36] Thus, even though different depths were analyzed, we found no signal from polymeric Au(I)−TMA species. Therefore, the etching process was successfully suppressed under the particular conditions of our ligand-exchange reactions (2:1 Au:TMA molar ratio).

Figure 3 shows the S 2p regions of the TMA-modified gold nanoparticles prepared by ligand exchange reactions. The spectra have been fitted with the three components already described for thiol adsorption on flat surfaces. These particles

dx.doi.org/10.1021/la404674m | Langmuir 2014, 30, 1820−1826

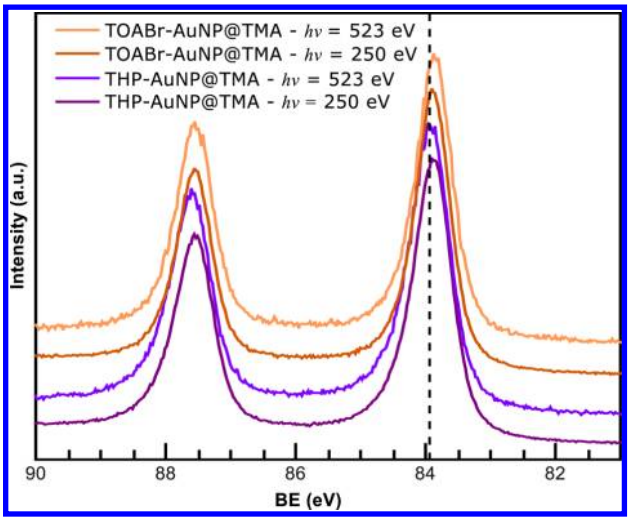

Figure 2. High-resolution Au 4f XPS spectra of THP-AuNP@TMA and TOABr-AuNP@TMA measured with a $h\nu$ = 250 and 523 eV. The vertical dashed line is located at 83.92 eV, the BE found for the Au $4f_{7/2}$ peak of a dodecanothiolate SAM on Au(111).

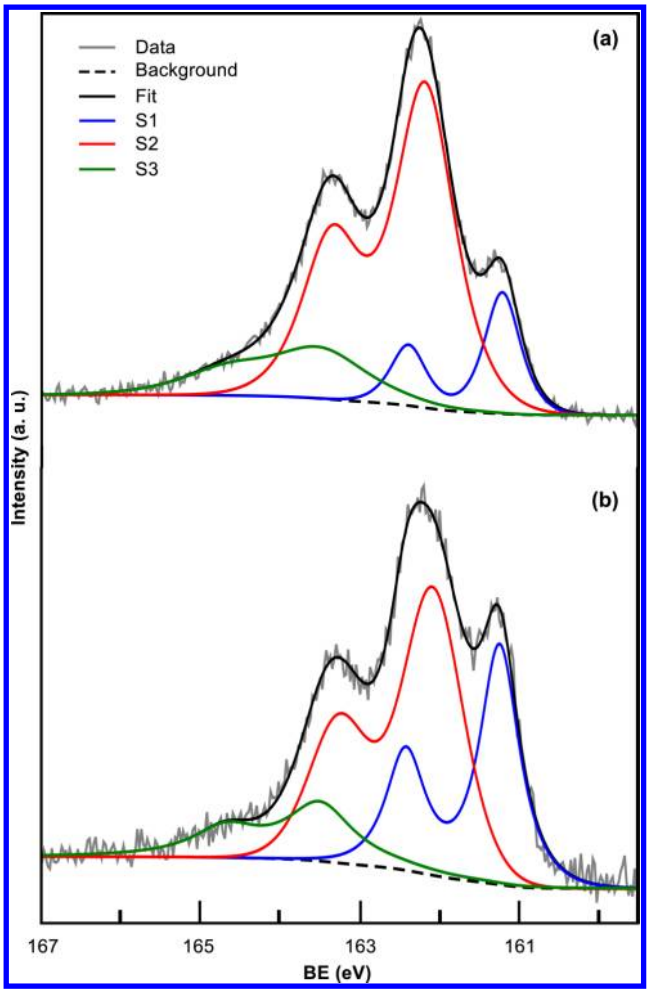

Figure 3. High-resolution S 2p XPS spectra of AuNPs protected by TMA, $h\nu$ = 250 eV. (a) THP-AuNP@TMA (S1: BE = 161.21 eV, fwhm = 0.53 eV; S2: BE = 162.18 eV, fwhm = 0.88 eV; S3: BE = 163.4 eV). The relative amounts of S1 and S2 were 18.7% and 81.3%, respectively. (b) TOABr-AuNP@TMA (S1: BE = 161.24 eV, fwhm = 0.56 eV; S2: BE = 162.07 eV, fwhm = 0.90 eV; S3: BE = 163.4 eV). The relative amounts of S1 and S2 were 38.2% and 61.8%, respectively.

exhibit higher amounts of atomic sulfur than that observed on Au(111). We found two feasible explanations for the origin of this species. We analyzed whether the atomic sulfur is formed upon TMA adsorption but also considered its presence as a consequence of radiation damage during XPS measurements. In this regard, Gonella et al.[37] reported that the long irradiation time of 3-mercaptopropionic acid SAMs on Au(111) leads to the development of the component at 161 eV. However, under our experimental conditions extensive X-ray exposure leads to an increase in the S3 signal, at expenses of the S1 and S2 components (see Supporting Information). The same trend has been observed on studies of radiation damage on dodecanethiolate SAMs on Au by Laiho et al.[38] Thus, we consider that atomic sulfur forms upon TMA adsorption and not as a consequence of radiation damage.

It is important to note that for gold@gold(I)-thiomalate core@shell nanoparticles obtained by the traditional one-phase synthesis[8] the binding energy values of sulfur and thiolate are different from those reported in this paper because these species are in a different environment. In that case most of the atomic sulfur and thiolate species are bonded to Au(I) species, and higher binding energies are expected.[39,40] On the contrary, the nanoparticles prepared by ligand-exchange reaction with a limited amount of TMA lead to BEs consistent with adsorption of sulfur species on metallic Au.

The analysis of the C 1s signal is useful to hold the idea that the S2 signal comes from the thiomalate adsorbed on Au sites. Figure 4 shows the high-resolution XPS spectrum of C 1s region of THP-AuNP@TMA ($h\nu$ = 523 eV), where five components were used to fit the data. The C5 peak was assigned to carboxylic groups. The C4 was related to the carbon bonded to sulfur,[37,41] while C3 was associated with the methylene group. As expected for TMA, both C5:C4 and C5:C3 ratios resulted very close to 2:1. These results show that the TMA molecules adsorb as thiolates, although some intact TMA molecules are also present as proposed from the analysis of the S 2p signal. In other words, molecular fragmentation should not be significant during spectra acquisition. Additionally, the C5 peak was used to estimate the COOH:S atomic ratio, considering the contributions from S2 and S3. For the two kinds of TMA-protected particles, the COOH:S atomic ratio was estimated considering the peak areas, the atomic subshell photoionization cross sections,[42] the angular asymmetry factor,[35] and the attenuation of the S signal due to the TMA residue[43−45] (for more details see Supporting Information). We obtained C5:(S2 + S3) ratios of 1.5:1 for THP-AuNP@TMA and 1.7:1 for TOABr-AuNP@TMA. Considering that all of the available models overestimate the electron attenuation by the carbon chain, these stoichiometry ratios are in good agreement with the expected value 2:1 for TMA and thiomalate. However, if the three sulfur components are taken into account, the C5:(S1 + S2 + S3) ratios resulted in 1.3 and 1.1 for THP-AuNP@TMA and TOABr-AuNP@TMA, respectively. Thus, these results support the idea that S1 correspond to atomic sulfur.

The reason Au nanoparticles present a higher proportion of atomic sulfur than SAMs of TMA on flat gold might be in the high amount of defect sites on nanoparticles with enhanced activity for the formation of atomic S in a heterogeneous cleavage process.[46] Additionally, the TMA molecule seems to be prone to experience S−C bond scission in comparison with other thiols. Indeed, AuNPs protected with 3-mercaptopro-

dx.doi.org/10.1021/la404674m | Langmuir 2014, 30, 1820−1826

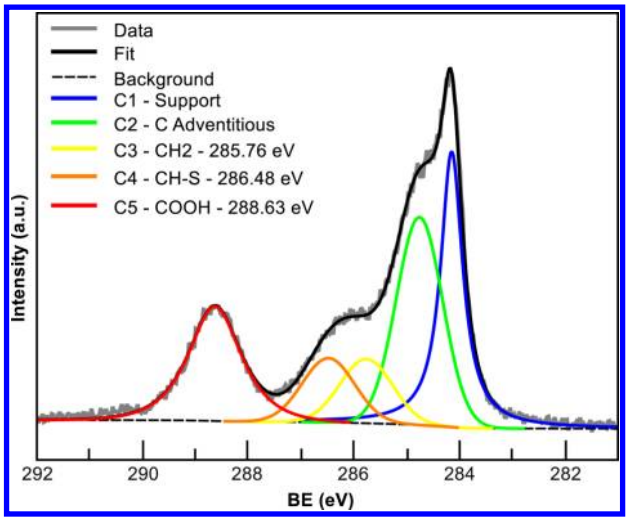

Figure 4. High-resolution C 1s XPS spectrum of THP-AuNP@TMA ($h\nu$ = 523 eV). The spectrum was fitted with five peaks: C1 comes from the support; C2 is the typical adventitious carbon; C3 and C4, of similar areas, are associated with the methylene carbon and carbon bonded to S, respectively. C5 is assigned to carbon of carboxylic groups.

pionic acid, also prepared by ligand exchange, do not show atomic sulfur species (see XPS data in the Supporting Information).

The C−S bond cleavage have been reported for the adsorption of other thiols on planar or nanoparticle surfaces.[30,47,48] As well as TMA, those thiols have electron-withdrawing groups or a double bond close to the C−S bond. The tendency of thiols to suffer C−S bond scission can rely on different factors. The proximity of the carboxylic acid function affects the strength of the C−S bond. Then, we have estimated the frequency of the normal vibration mode that implies the elongation of the C−S bond in different molecules. For C−S elongation in mercaptoacetic acid, the normal vibrational frequency is lower than that calculated for 3-mercaptopropionic acid. In the case of the TMA molecule (nearest carboxylic acid function in the α-position with respect to C−S bond), the frequency of this mode is lower than that for 2-(mercaptomethyl)succinic acid (nearest carboxylic acid function in the β-position) (see Supporting Information). This observation is supported considering that electron-withdrawing groups in the α-position will result in the formation of better leaving groups. Additionally, significant electron-charge transfer from the surface of gold nanoparticles to the sulfur atoms of the thiolates has been proposed based on X-ray absorption near-edge structure (XANES) data.[49] Taking into account the above discussion, the molecular structure of the TMA and our experimental results we propose a cleavage mechanism where (i) S withdraws charge form gold surface and (ii) the negatively charged leaving group is partially stabilized by electronic resonance with the carboxylic group at α position to C−S bond (Scheme 1).

This mechanism is supported by the higher amount of atomic sulfur found in the TOABr-AuNP@TMA, in comparison with THP-AuNP@TMA. During ligand exchange reaction the tetraoctylammonium cations present on the nanoparticle surface could form ionic pairs with the negatively charged leaving groups. This might minimize the energy barrier of the cleavage process.

Scheme 1. (a) Proposed Mechanism of C−S Cleavage;[a] (b, c) Schematic Representations of Ligand Exchange Reactions[b]

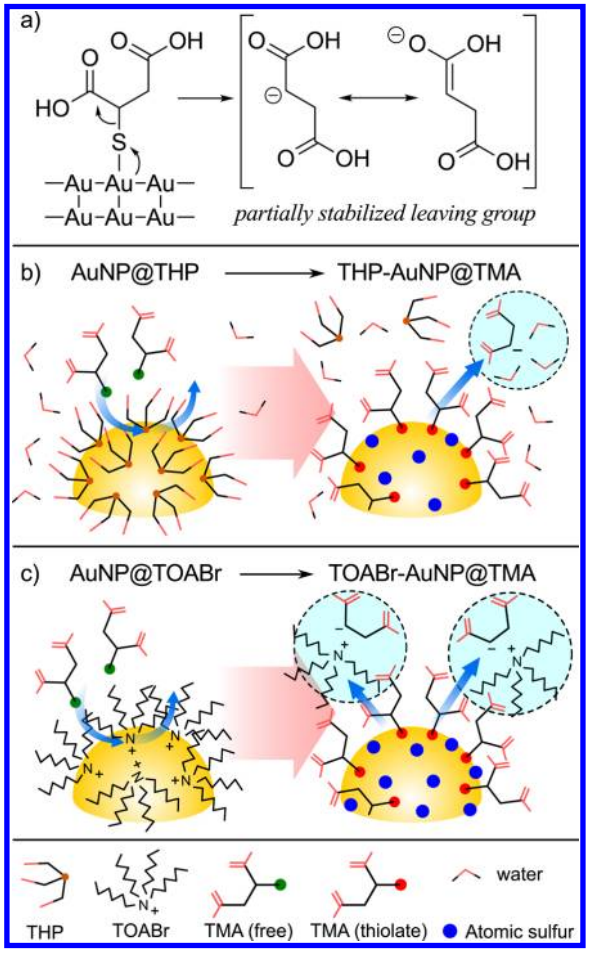

[a]The sulfur atom takes charge from gold, and the carboxylic group weakens the C−S bond. The negatively charged leaving group is partially stabilized by electronic resonance. [b]The light blue circles show the stabilization processes for the leaving group. In panel c, the high concentration of cations near the surface favors the C−S bond scission, increasing the amount of atomic sulfur.

CONCLUSIONS

Thiomalic acid forms thiomalate self-assembled monolayers when it is adsorbed on Au(111) surfaces. On these planar substrates the thiolate coverage is lower than that found for alkanethiols, which was explained considering steric hindrance. Additionally, low coverages of atomic sulfur were confirmed from both XPS and electrochemical data.

Also, thiomalic acid adsorbs mainly as thiomalate onto preformed Au nanoparticles protected by labile ligands. However, the amount of atomic sulfur is higher than that found on the Au(111) surface. This is related to the higher density of surface defects on the nanoparticles when compared with Au(111). Furthermore, the extent of the C−S bond cleavage seems to depend on the ability of the media to stabilize the anionic leaving group,. The electron-withdrawing ability of the carboxylic group in the α-position with respect to the C−S bond gives additional stability to the leaving group. Additionally, the C−S bond scission is favored when tetraalkylammonium cations are adsorbed on the surface of the Au nanoparticles.

dx.doi.org/10.1021/la404674m | Langmuir 2014, 30, 1820−1826

Finally, the ligand exchange reactions lead to nanoparticles formed by Au(0), different from those obtained by the traditional synthesis in polar media which are mainly composed by Au(I) species. In the latter case, the Au(I)−thiolate intermediates are kinetically trapped and cannot be fully reduced to Au(0). Furthermore, the thiomalic acid-protected Au nanoparticles can be dispersed in aqueous solution in a wide range of pHs, from 1 to 13.

■ ASSOCIATED CONTENT

Supporting Information

Details of the TEM imaging, fitting of size distributions, XPS measurements, the calculation of the COOH/S ratio, the XPS analysis of AuNPs capped with 3-mercaptopropionic acid, computational methods for the calculation of the Vibration Frequencies, as well as the extension and characteristics of radiation induced damage are included in the Supporting Information. This material is available free of charge via the Internet at http://pubs.acs.org.

■ AUTHOR INFORMATION

Corresponding Authors

*Fax +54 221 425 4642; Ph +54 221 425 7430; e-mail mfonti@inifta.unlp.edu.ar (M.H.F.).

*Fax +54 221 425 4642; Ph +54 221 425 7430; e-mail rubert@quimica.unlp.edu.ar (A.R.).

Present Address

G.C.: Max Planck Institute for the Structure and Dynamics of Matter, Luruper Chaussee 149, 22761 Hamburg, Germany.

Notes

The authors declare no competing financial interest.

■ ACKNOWLEDGMENTS

This work was supported by "Agencia Nacional de Promoción Científica y Tecnológica" (PICT 2010-0423, PICT 2010-2554, PRH-74), CONICET (PIP 11220090100139), the National University of La Plata, Laboratório Nacional de Luz Síncrotron (LNLS), Campinas, Brazil (Research Proposals SGM-14387 and SGM-14243). J.C.A. is a doctoral fellow of CONICET.

■ REFERENCES

(1) Wei, J.; Liu, H.; Dick, A. R.; Yamamoto, H.; He, Y.; Waldeck, D. H. Direct Wiring of Cytochrome C's Heme Unit to an Electrode: Electrochemical Studies. *J. Am. Chem. Soc.* **2002**, *124*, 9591−9599.

(2) Królikowska, A.; Bukowska, J. Self-Assembled Monolayers of Mercaptosuccinic Acid Monolayers on Silver and Gold Surfaces Designed for Protein Binding. Part II: Vibrational Spectroscopy Studies on Cytochromec Immobilization. *J. Raman Spectrosc.* **2007**, *38*, 943−949.

(3) Ying, E.; Li, D.; Guo, S.; Dong, S.; Wang, J. Synthesis and Bio-Imaging Application of Highly Luminescent Mercaptosuccinic Acid-Coated CdTe Nanocrystals. *PLoS One* **2008**, *3*, e2222.

(4) Pensa, E.; Cortés, E.; Corthey, G.; Carro, P.; Vericat, C.; Fonticelli, M. H.; Benítez, G.; Rubert, A. A.; Salvarezza, R. C. The Chemistry of the Sulfur−Gold Interface: In Search of a Unified Model. *Acc. Chem. Res.* **2012**, *45*, 1183−1192.

(5) Azcárate, J. C.; Corthey, G.; Pensa, E.; Vericat, C.; Fonticelli, M. H.; Salvarezza, R. C.; Carro, P. Understanding the Surface Chemistry of Thiolate-Protected Metallic Nanoparticles. *J. Phys. Chem. Lett.* **2013**, 3127−3138.

(6) Chen, S.; Kimura, K. Synthesis and Characterization of Carboxylate-Modified Gold Nanoparticle Powders Dispersible in Water. *Langmuir* **1999**, *15*, 1075−1082.

(7) Ackerson, C. J.; Jadzinsky, P. D.; Kornberg, R. D. Thiolate Ligands for Synthesis of Water-Soluble Gold Clusters. *J. Am. Chem. Soc.* **2005**, *127*, 6550−6551.

(8) Corthey, G.; Giovanetti, L. J.; Ramallo-López, J. M.; Zelaya, E.; Rubert, A. A.; Benitez, G. A.; Requejo, F. G.; Fonticelli, M. H.; Salvarezza, R. C. Synthesis and Characterization of Gold@Gold(I)−Thiomalate Core@Shell Nanoparticles. *ACS Nano* **2010**, *4*, 3413−3421.

(9) Duff, D. G.; Baiker, A.; Edwards, P. P. A New Hydrosol of Gold Clusters. 1. Formation and Particle Size Variation. *Langmuir* **1993**, *9*, 2301−2309.

(10) Fink, J.; Kiely, C. J.; Bethell, D.; Schiffrin, D. J. Self-Organization of Nanosized Gold Particles. *Chem. Mater.* **1998**, *10*, 922−926.

(11) Jose, D.; Matthiesen, J. E.; Parsons, C.; Sorensen, C. M.; Klabunde, K. J. Size Focusing of Nanoparticles by Thermodynamic Control through Ligand Interactions. Molecular Clusters Compared with Nanoparticles of Metals. *J. Phys. Chem. Lett.* **2012**, *3*, 885−890.

(12) Fonticelli, M.; Azzaroni, O.; Benítez, G.; Martins, M. E.; Carro, P.; Salvarezza, R. C. Molecular Self-Assembly on Ultrathin Metallic Surfaces: Alkanethiolate Monolayers on Ag(1 × 1)−Au(111). *J. Phys. Chem. B* **2004**, *108*, 1898−1905.

(13) Abramoff, M. D.; Magalhães, P. J.; Ram, S. J. Image Processing with ImageJ. *Biophotonics Int.* **2004**, *11*, 36−42.

(14) Granqvist, C. G.; Buhrman, R. A. Ultrafine Metal Particles. *J. Appl. Phys.* **1976**, *47*, 2200−2219.

(15) Zharnikov, M. High-Resolution X-Ray Photoelectron Spectroscopy in Studies of Self-Assembled Organic Monolayers. *J. Electron Spectrosc. Relat. Phenom.* **2010**, *178−179*, 380−393.

(16) Allouche, A.-R. Gabedit—A Graphical User Interface for Computational Chemistry Softwares. *J. Comput. Chem.* **2011**, *32*, 174−182.

(17) Stewart, J. J. P. *MOPAC2012*, Stewart Computational Chemistry, Colorado Springs, CO, 2012.

(18) Janssen, C.; Seidl, E.; Colvin, M. Object-Oriented Implementation of Parallel Ab Initio Programs. *ACS Symp. Ser.* **1995**, *592*.

(19) Janssen, C. L.; Nielsen, I. B.; Leininger, M. L.; Valeev, E. F.; Seidl, E. T. *The Massively Parallel Quantum Chemistry Program (MPQC)*; Sandia National Laboratories: Livermore, CA, 2004.

(20) Stewart, J. J. P. Optimization of Parameters for Semiempirical Methods V: Modification of NDDO Approximations and Application to 70 Elements. *J. Mol. Model.* **2007**, *13*, 1173−1213.

(21) Vericat, C.; Vela, M. E.; Benitez, G.; Carro, P.; Salvarezza, R. C. Self-Assembled Monolayers of Thiols and Dithiols on Gold: New Challenges for a Well-Known System. *Chem. Soc. Rev.* **2010**, *39*, 1805−1834.

(22) Fonticelli, M. H.; Benitez, G.; Carro, P.; Azzaroni, O.; Salvarezza, R. C.; Gonzalez, S.; Torres, D.; Illas, F. Effect of Ag Adatoms on High-Coverage Alkanethiolate Adsorption on Au(111). *J. Phys. Chem. C* **2008**, *112*, 4557−4563.

(23) Azzaroni, O.; Vela, M. E.; Martin, H.; Hernández Creus, A.; Andreasen, G.; Salvarezza, R. C. Electrodesorption Kinetics and Molecular Interactions at Negatively Charged Self-Assembled Thiol Monolayers in Electrolyte Solutions. *Langmuir* **2001**, *17*, 6647−6654.

(24) Ramírez, E. A.; Cortés, E.; Rubert, A. A.; Carro, P.; Benítez, G.; Vela, M. E.; Salvarezza, R. C. Complex Surface Chemistry of 4-Mercaptopyridine Self-Assembled Monolayers on Au(111). *Langmuir* **2012**, *28*, 6839−6847.

(25) Vericat, C.; Andreasen, G.; Vela, M. E.; Salvarezza, R. C. Dynamics of Potential-Dependent Transformations in Sulfur Adlayers on Au(111) Electrodes. *J. Phys. Chem. B* **2000**, *104*, 302−307.

(26) Vericat, C.; Vela, M. E.; Benitez, G. A.; Gago, J. A. M.; Torrelles, X.; Salvarezza, R. C. Surface Characterization of Sulfur and Alkanethiol Self-Assembled Monolayers on Au(111). *J. Phys.: Condens. Matter* **2006**, *18*, R867.

(27) Yang, Y. W.; Fan, L. J.; High-Resolution, X. P. S. Study of Decanethiol on Au(111): Single Sulfur−Gold Bonding Interaction. *Langmuir* **2002**, *18*, 1157−1164.

(28) Heister, K.; Zharnikov, M.; Grunze, M.; Johansson, L. S. O.; Ulman, A. Characterization of X-Ray Induced Damage in Alkanethio-

late Monolayers by High-Resolution Photoelectron Spectroscopy. *Langmuir* **2001**, *17*, 8−11.
(29) Zhong, C.-J.; Brush, R. C.; Anderegg, J.; Porter, M. D. Organosulfur Monolayers at Gold Surfaces: Reexamination of the Case for Sulfide Adsorption and Implications to the Formation of Monolayers from Thiols and Disulfides. *Langmuir* **1999**, *15*, 518−525.
(30) Ishida, T.; Choi, N.; Mizutani, W.; Tokumoto, H.; Kojima, I.; Azehara, H.; Hokari, H.; Akiba, U.; Fujihira, M. High-Resolution X-Ray Photoelectron Spectra of Organosulfur Monolayers on Au(111): S(2p) Spectral Dependence on Molecular Species. *Langmuir* **1999**, *15*, 6799−6806.
(31) Fischer, J. A.; Zoldan, V. C.; Benitez, G.; Rubert, A. A.; Ramirez, E. A.; Carro, P.; Salvarezza, R. C.; Pasa, A. A.; Vela, M. E. Sulfidization of Au(111) from Thioacetic Acid: An Experimental and Theoretical Study. *Langmuir* **2012**, *28*, 15278−15285.
(32) Hayashi, T.; Wakamatsu, K.; Ito, E.; Hara, M. Effect of Steric Hindrance on Desorption Processes of Alkanethiols on Au(111). *J. Phys. Chem. C* **2009**, *113*, 18795−18799.
(33) Hinterwirth, H.; Kappel, S.; Waitz, T.; Prohaska, T.; Lindner, W.; Lämmerhofer, M. Quantifying Thiol Ligand Density of Self-Assembled Monolayers on Gold Nanoparticles by Inductively Coupled Plasma−Mass Spectrometry. *ACS Nano* **2013**, *7*, 1129−1136.
(34) Toikkanen, O.; Ruiz, V.; Rönnholm, G.; Kalkkinen, N.; Liljeroth, P.; Quinn, B. M. Synthesis and Stability of Monolayer-Protected Au_{38} Clusters. *J. Am. Chem. Soc.* **2008**, *130*, 11049−11055.
(35) Briggs, D.; Seah, M. P. *Practical Surface Analysis: By Auger and X-Ray Photoelectron Spectroscopy*; Wiley: Chichester, 1990.
(36) Cumpson, P. J.; Seah, M. P. Elastic Scattering Corrections in AES and XPS. II. Estimating Attenuation Lengths and Conditions Required for Their Valid Use in Overlayer/Substrate Experiments. *Surf. Interface Anal.* **1997**, *25*, 430−446.
(37) Gonella, G.; Cavalleri, O.; Terreni, S.; Cvetko, D.; Floreano, L.; Morgante, A.; Canepa, M.; Rolandi, R. High Resolution X-Ray Photoelectron Spectroscopy of 3-Mercaptopropionic Acid Self-Assembled Films. *Surf. Sci.* **2004**, *566−568* (Part 1), 638−643.
(38) Laiho, T.; Leiro, J. .; Lukkari, J. XPS Study of Irradiation Damage and Different Metal−sulfur Bonds in Dodecanethiol Monolayers on Gold and Platinum Surfaces. *Appl. Surf. Sci.* **2003**, *212−213*, 525−529.
(39) Bourg, M.-C.; Badia, A.; Lennox, R. B. Gold−Sulfur Bonding in 2D and 3D Self-Assembled Monolayers: XPS Characterization. *J. Phys. Chem. B* **2000**, *104*, 6562−6567.
(40) Walton, R. A. The X-Ray Photoelectron Spectra of Metal Complexes of Sulfur-Containing Ligands: Sulfur 2p Binding Energies. *Coord. Chem. Rev.* **1980**, *31*, 183−220.
(41) Whelan, C. M.; Smyth, M. R.; Barnes, C. J. HREELS, XPS, and Electrochemical Study of Benzenethiol Adsorption on Au(111). *Langmuir* **1999**, *15*, 116−126.
(42) Yeh, J. J.; Lindau, I. Atomic Subshell Photoionization Cross Sections and Asymmetry Parameters: 1 < Z < 103. *At. Data Nucl. Data Tables* **1985**, *32*, 1−155.
(43) Laibinis, P. E.; Bain, C. D.; Whitesides, G. M. Attenuation of Photoelectrons in Monolayers of N-Alkanethiols Adsorbed on Copper, Silver, and Gold. *J. Phys. Chem.* **1991**, *95*, 7017−7021.
(44) Snow, A. W.; Jernigan, G. G.; Ancona, M. G. Packing Density of $HS(CH_2)_nCOOH$ Self-Assembled Monolayers. *Analyst* **2011**, *136*, 4935−4949.
(45) Seah, M. P. Simple Universal Curve for the Energy-Dependent Electron Attenuation Length for All Materials: Simple, Accurate, Universal Expression for Attenuation Lengths. *Surf. Interface Anal.* **2012**, *44*, 1353−1359.
(46) Janssens, T. V. W.; Clausen, B. S.; Hvolbæk, B.; Falsig, H.; Christensen, C. H.; Bligaard, T.; Nørskov, J. K. Insights into the Reactivity of Supported Au Nanoparticles: Combining Theory and Experiments. *Top. Catal.* **2007**, *44*, 15−26.
(47) Houmam, A.; Muhammad, H.; Koczkur, K. M. Rapid Formation of a Dense Sulfur Layer on Gold through Use of Triphenylmethane Sulfenyl Chloride as a Precursor. *Langmuir* **2012**, *28*, 16881−16889.
(48) Battocchio, C.; Meneghini, C.; Fratoddi, I.; Venditti, I.; Russo, M. V.; Aquilanti, G.; Maurizio, C.; Bondino, F.; Matassa, R.; Rossi, M.; et al. Silver Nanoparticles Stabilized with Thiols: A Close Look at the Local Chemistry and Chemical Structure. *J. Phys. Chem. C* **2012**, *116*, 19571−19578.
(49) Jiang, Y.; Yin, P.; Li, Y.; Sun, Z.; Liu, Q.; Yao, T.; Cheng, H.; Hu, F.; Xie, Z.; He, B.; et al. Modifying the Atomic and Electronic Structures of Gold Nanocrystals via Changing the Chain Length of N-Alkanethiol Ligands. *J. Phys. Chem. C* **2012**, *116*, 24999−25003.